

REVIEW ARTICLE

The Development of High Oxygen Pressures and the Stabilization of Unusual Oxidation States of Transition Metals

G rard DEMAZEAU

*Institut de Chimie de la Mati re Condens e Bordeaux I.C.M.C.B.-C.N.R.S. UPR 9048
Avenue du Dr. A. Schweitzer-33608 Pessac Cedex France and Interface Hautes
Pressions-E.N.S.C.P.B. Avenue Pey-Berland-BP 108-33402 Talence Cedex France*

(Received October 21, 1997)

ABSTRACT. High oxygen pressures appear an important tool in Solid State Chemistry. Two main routes can be developed: (i) the stabilization of thermally unstable oxides, used as precursors, in order to open the synthesis of new materials, (ii) the stabilization of the highest oxidation states of transition metals. This paper is essentially devoted to this second research axis. The methodology developed for preparing new oxides containing Fe(V), Ir(VI), high spin Fe(IV) and Cu(III) is described.

INTRODUCTION

For a cation M^{n+} when the formal oxidation state $n+$ increases consequently the M-O distance decreases. Such a phenomenon induces an improvement of the covalence of this chemical bond leading to strong modifications of the physico-chemical properties of the corresponding oxide. Another interest for the stabilization of the highest $n+$ values is to compare the variation of the M-O distances versus n and the shrinking of the M-O distances when an oxide lattice is submitted to high pressures. The compressibility of solids being small compared to the gas and liquid phases, the M-O distances reach through the increase of $n+$ are probably smaller and consequently this stabilization of the highest oxidation states appears to be an interesting way for the study of oxides in extreme pressure conditions.

The stabilization of an unusual oxidation state of a transition metal is closely dependent on that of its corresponding electronic configuration, i.e. the repartition of the electrons in the corresponding d-orbitals. Consequently, the local structural and chemical factors characterizing the first oxygen polyhedron containing this transition metal play an important role. The thermodynamical parameters

(pressure and temperature) governing the synthesis of the oxygen lattice are also critical. High oxygen pressures help the formation of such a lattice ($A_{\text{solid}} + B_{\text{solid}} + m/2O_2 \rightarrow ABO_m$ with $\Delta G = \Delta G_0 - m/2RT \log pO_2$, if $pO_2 \nearrow \Delta G \searrow$). On the contrary, the use of high temperatures, very often required for improving the diffusion in the solid state, impede the stabilization of the highest valencies.¹

These different parameters will be studied and then some illustrations concerning the stabilization of Fe(IV), Fe(V), Ir(VI) and Cu(III) will be described.

ROLE OF THE LOCAL FACTORS CHARACTERIZING THE FIRST OXYGEN SURROUNDING OF A TRANSITION ELEMENT ON THE STABILIZATION OF AN UNUSUAL OXIDATION STATE

On the basis of a six-coordinated cation, a simple model based both on the Tanabe-Sugano diagrams² and the energy of the d-orbitals in different symmetries³ has led to foresee for a transition-cation M^{n+} the domain of stability of its different electronic configurations versus the local relative crystal field energy Dq/B and the local structural distortion [elongation $\theta = \{(M-O)_z\} / \{(M-O)_{xy}\}$

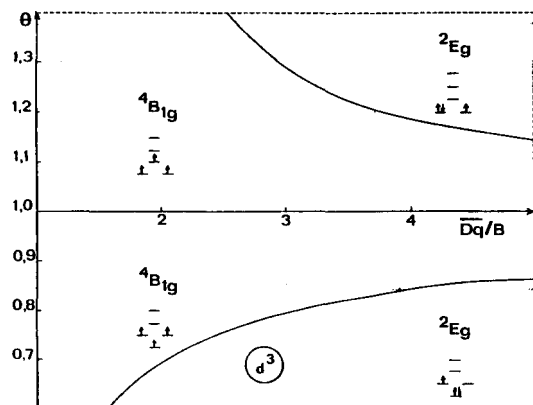


Fig. 1. Domains of stability (θ , $\overline{Dq/B}$) for the fundamental terms characterizing the electronic population d^3 in a D_{4h} symmetry.

> 1 or compression $\theta = \{(M-O)_z\} / \{(M-O)_{xy}\} < 1$.^{4,5}

This model was set up also on the basis on different approximations:

- the energy of the different terms varies linearly versus \overline{Dq} ,
- \overline{Dq} is a function of $d(M-O)$,⁵
- the spin-orbit coupling is neglected.

The Fig. 1, 2, 3 give respectively the resulting diagrams (θ , $\overline{Dq/B}$) corresponding to the electronic population d^3 , d^4 , d^8 associated to Fe(V), Ir(VI), Fe(IV) and Cu(III).

DEVELOPMENT OF HIGH OXYGEN PRESSURES

High oxygen pressures can be produced through three different ways¹:

1) The compression of oxygen gas till 5 kbar (500 MPa), but due to the external heating of the reaction vessel used, pressure and temperature are strongly correlated (500 MPa-600°C or 100 MPa-900°C are the extreme experimental conditions).

2) The development of oxidizing solutions (as diluted solutions of NH_4ClO_4), the extreme experimental conditions being approximately the same than that used for compressed oxygen.

3) The use of oxygen pressures in solid state through the thermal decomposition of unstable oxides. Instead of CrO_3 leading to ferromagnetic CrO_2 as resulting oxide, $KClO_3$ was developed ($KClO_3$

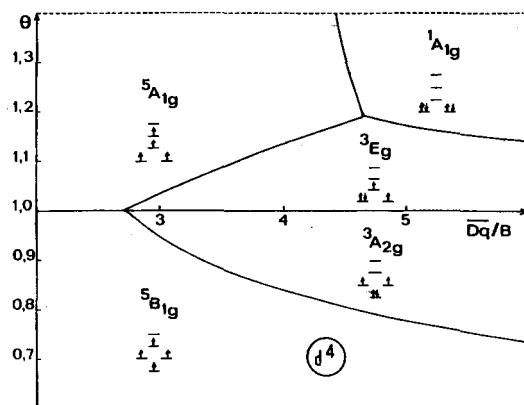


Fig. 2. Domains of stability (θ , $\overline{Dq/B}$) for the fundamental terms characterizing the electronic population d^4 in a D_{4h} symmetry.

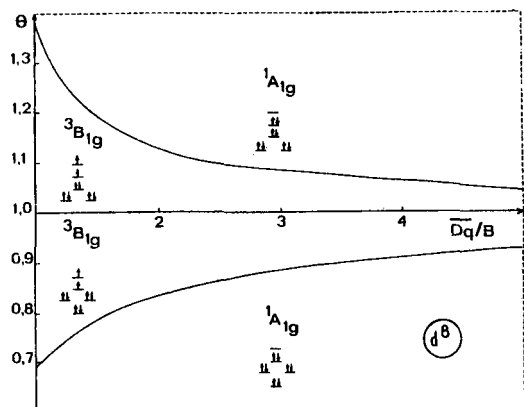


Fig. 3. Domains of stability (θ , $\overline{Dq/B}$) for the fundamental terms characterizing the electronic population d^8 in a D_{4h} symmetry.

$\rightarrow KCl + 3/2O_2$) as oxygen source. This thermally unstable oxide is intimately mixed with the reactants in order to prevent all inhomogeneity of oxygen composition in the final material. Such a method allows to reach the highest oxygen pressures and temperatures (8 GPa-2000°C).

STABILIZATION OF SIX-COORDINATED Fe(V) IN AN OXYGEN LATTICE

Selection of the local factors (structural and chemical) able to help such a stabilization. If six-coordinated Fe(V) can exist in an oxygen lattice, due to its isotropic electronic configuration $t_{2g}^6 e_g^0$, such an oxidation state can be stabilized in a

site with a pure local O_h symmetry. Consequently, it is necessary to select an appropriate lattice characterized both by six-coordinated sites with a pure octahedral symmetry (O_h) and stable under high pressure conditions (the stabilization of Fe(V) requiring probably high oxygen pressures). The best structure corresponding to these criteria appears to be the perovskite one (ABO_3).

On the basis of the stabilization of Fe(V) in such a perovskite lattice the resulting Fe(V)-O bond would be very strong. Consequently all increase of the covalency of the Fe-O bond in the ABO_3 lattice will improve the stabilization of the highest oxidation state. In the perovskite lattice the B-O-B angle between two consecutive B-O bonds is equal to 18° and the same 2p orbital of oxygen is shared between two competing B-O bonds. In order to reinforce the covalency of the B-O bond, it is possible to select as competing B'-O bond a weak one. Of course, in such a case, the chemical formula of the resulting perovskite is $A_2BB'O_6$. In order to satisfy such a criteria, a weak B'-O bond, as Li-O, has been selected $\{A_2Fe(V)Li(I)O_6\}$.

The A cation is optimized according to two criteria (i) the equilibrium of the cationic and anionic charges (A^{3+}) and (ii) its size in order to maintain the local O_h symmetry for the (FeO_6) polyhedron. On these basis La(III) was selected. At the end of this first step, the La_2LiFeO_6 stoichiometry appears to be

very appropriated for helping the stabilization of Fe(V).

Preparation of La_2LiFeO_6 . The second step consisted on the optimization of the thermodynamical conditions: temperature and oxygen pressure able to lead to a pure stoichiometric phase. La_2LiFeO_6 was prepared in two steps. The first consisted on the calcination of the corresponding nitrates $\{La(NO_3)_3, LiNO_3 \text{ and } Fe(NO_3)_3\}$ in the stoichiometric ratio {only an excess of $LiNO_3$ ($\approx 30-50\%$) is used in order to prevent the sublimation of the resulting Li_2O before the chemical reaction}. The second step was a treatment under high oxygen pressures. Using the thermal decomposition of $KClO_3$ as oxygen source in a belt-type apparatus¹ at 60 kbar (6 GPa) and a temperature close to $900^\circ C$, 15 min. are only necessary for preparing a pure phase (from X-ray diffraction analysis).⁶

Physico-chemical characterizations of La_2LiFeO_6 . The oxidation state of iron was obtained from a oxidation-reduction titration. The resulting value (5.02 ± 0.05) confirms the stoichiometry La_2LiFeO_6 . The main results issued from the selected physical characterizations (X-ray diffraction analysis, magnetic measurements, Mössbauer spectroscopy) are summarized in Table 1. All the experimental values confirmed the stabilization of six-coordinated Fe(V) in an oxygen lattice. The evolution of the Fe^{n+} -O distance versus the increase of the n value (n=II, III, IV, V) is given on Table 2. The

Table 1. Physical characterizations of the La_2LiFeO_6 oxide₆

X.R.D.	Perovskite structure with a small rhombohedral distortion, 1/1 Li/Fe cationic ordering, $d(Fe-O)=1.86 \text{ \AA}$ (from neutronic diffraction analysis)	$a_c = 5.371 \text{ \AA}$ $\alpha = 60.66^\circ$
Magnetic measurement	Antiferromagnetic behaviour at low temperature, Curie-Weiss behaviour at highest temperature	$T_N \approx 10 \text{ K}$, $C_{exp} \approx 1.93$ $C_{theor.} = 1.875 \left(\frac{1}{2}g\right)^2$
Mössbauer spectroscopy	Isomer shift δ/Fe_n (at 293 K) = $-0.41 \pm 0.01 \text{ mm/s}$ $\Gamma = 0.26 \pm 0.01 \text{ mm/s}$	
E.P.R. measurements	g_{exp} (293 K) = 2.0135 ± 0.0001 g (293 K) observed for $SrTiO_3:Fe^{5+}$ $g = 2.0131^7$	

Table 2. Evolution of the Fe^{n+} -O distance versus the formal n+ value ($r(Fe^{n+})$ is defined on the basis of $r(O^{2-})=1.40 \text{ \AA}$)

	Fe(III)-O ($LiFeO_2$)	Fe(IV)-O ($Sr_{0.50}La_{1.50}Li_{0.50}Fe_{0.50}O_4$)	Fe(V)-O (La_2LiFeO_6)
Fe^{n+} -O (\AA)	2.03	1.95 ₆	1.86
$r(Fe^{n+})$ (\AA)	0.63	0.55 ₆	0.46

Table 3. Synthesis under oxygen pressures of different oxides with the perovskite structure and containing Ir(VI)¹⁰

General formula	Ref.	T (�C)	P	Time	Ir oxidation state from chemical titration
Ba ₂ CaIrO ₆	11, 12	880	60 MPa	48 h	5.99
		900	6 GPa	10 min.	6.00
BaSrIrO ₆	12	880	60 MPa	48 h	5.88
Ba ₂ ZnIrO ₆	13	1000	7 GPa	15 min.	5.96
Sr ₂ CaIrO ₆	14	880	60 MPa	48 h	5.98
Sr ₂ MgIrO ₆	14	900	6 GPa	5 min.	5.81
Sr ₂ ZnIrO ₆	13	1000	7 GPa	15 min.	5.72
BaLaLiIrO ₆	15	800	7.5 GPa	15 min.	5.98

evaluated ionic radius for Fe(V) is close to 0.46  . More recently Fe(V) has been stabilized in a double perovskite La₂LiV_{1-x}Fe_xO₆.⁸

STABILIZATION OF SIX-COORDINATED Ir(VI) IN AN OXIDE LATTICE

Ir(VI) in an octahedral coordination has the same electronic configuration (*t*_{2g}⁶) that Fe(V). Developing the same methodology, Ir(VI) has been recently stabilized in different oxygen lattices with the perovskite structure.¹⁰ Table 3 gives the different Ir(VI) oxides stabilized under oxygen pressures. The physical characterizations of such iridium oxides confirm the stabilization of Ir(VI).

Table 4. Structural results concerning the Ir(VI) perovskites¹⁰

X-ray diffraction analysis	
Ba ₂ CaIrO ₆	Cubic perovskite a=8.364±0.001 �
Ba ₂ SrIrO ₆	Rhombohedral perovskite a=6.025±0.001 � α=60.48±0.01�
Ba ₂ ZnIrO ₆	Cubic perovskite a=8.103±0.001 �
Sr ₂ CaIrO ₆	Monoclinic distortion a=5.783±0.001 � b=5.828±0.001 � c=8.200±0.001 � β=90.26±0.01�
Sr ₂ ZnIrO ₆	Cubic perovskite a=7.932±0.001 �
Sr ₂ MgIrO ₆	Cubic perovskite a=7.891±0.001 �
BaLaLiIrO ₆	Cubic perovskite a=7.947±0.001 �

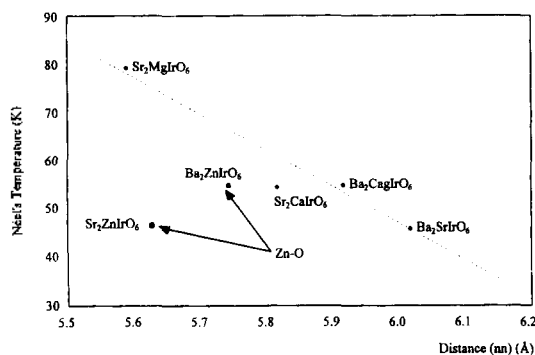


Fig. 4. Correlations between the Ir(VI)-Ir(VI) distance and the observed *T_N* values for the oxides A₂MIr(VI)O₆ with the perovskite structure (A=Ba, Sr, M=Sr, Ca, Mg, Zn).

The main structural results are given on Table 4. The evolution of the *T_N* values versus the Ir-Ir distance is observed on the Fig. 4. Due to the super-superexchange interaction between two Ir(VI), the *T_N* value increases drastically with the shrinking of the Ir-Ir distance. The variation of the isomer shift of Irⁿ⁺ versus the n+ value on the Fig. 5.¹¹

Recently, through Ir-L_{III} edge XANES study of these Ir(VI) perovskites, an evaluation of the energy splitting between the *t*_{2g} and *e_g* level has been obtained.¹⁶ The variation of such a splitting versus the n+ oxidation state has been evaluated for different iridium oxides with the perovskite structure (Table 5). This splitting increases with the n+ value from Ir(IV) to Ir(VI) but its value is also closely dependent on the strength of the competing bond.

STABILIZATION OF Fe(IV) WITH THE HIGH SPIN CONFIGURATION

Fe(IV) (*d*⁴) can present the high spin state

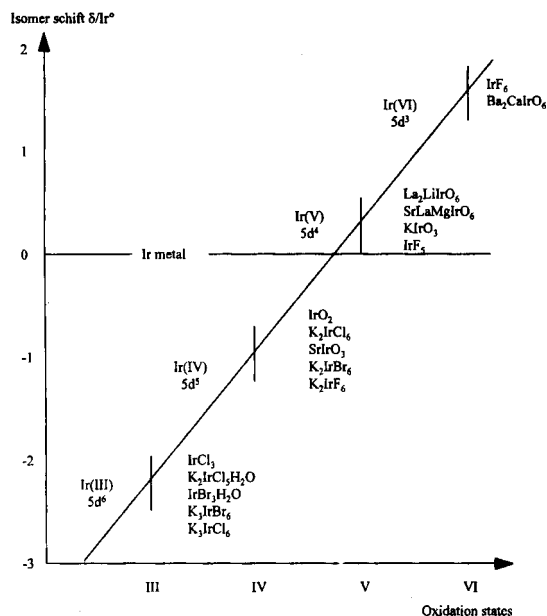


Fig. 5. Isomer shift δ/ir° for Ir with different oxidation states in oxides or halogenated compounds.

Table 5. Evaluation of the energy splitting ($t_{2g}-e_g$) for different iridium oxides¹⁶

Compounds	n+	($t_{2g}-e_g$) splitting (eV)
$\text{La}_2\text{ZnIrO}_6$	IV	3.05
$\text{La}_2\text{MgIrO}_6$	IV	3.18
Ba_2YIrO_6	V	3.26
$\text{La}_2\text{LiIrO}_6$	V	3.67
BaLaLiIrO_6	VI	3.85
$\text{Ba}_2\text{ZnIrO}_6$	VI	3.16
$\text{Ba}_2\text{CaIrO}_6$	VI	3.88

($t_{2g}^3 d_{xy}^2 d_{x^2-y^2}^0$) in a strongly elongated octahedron (Fig. 2). The Fig. 6 gives the selection of the local structural and chemical factors leading to the proposed stoichiometry $\text{A}_{0.50}\text{La}_{1.50}\text{Li}_{0.50}\text{Fe(IV)}_{0.50}\text{O}_4$ (A = Ca, Sr, Ba). Using high oxygen pressures such oxides has been prepared and characterized.¹⁷⁻²⁰

Table 6. Physical characterizations of the oxides $\text{A}_{0.50}\text{La}_{1.50}\text{Li}_{0.50}\text{Fe}_{0.50}\text{O}_4$ (A=Ca, Sr, Ba)

	Experimental Curie constant	T_N (K)	$\bar{\delta}/\alpha$ Fe mm/s (293 K)	$\bar{\Delta}$ mm/s
$\text{Ca}_{0.50}\text{La}_{1.50}\text{Li}_{0.50}\text{Fe}_{0.50}\text{O}_4$	3.09	35	-0.20	1.07
$\text{Sr}_{0.50}\text{La}_{1.50}\text{Li}_{0.50}\text{Fe}_{0.50}\text{O}_4$	3.06	32	-0.18	1.13
$\text{Ba}_{0.50}\text{La}_{1.50}\text{Li}_{0.50}\text{Fe}_{0.50}\text{O}_4$	3.02	28	-0.17	1.03

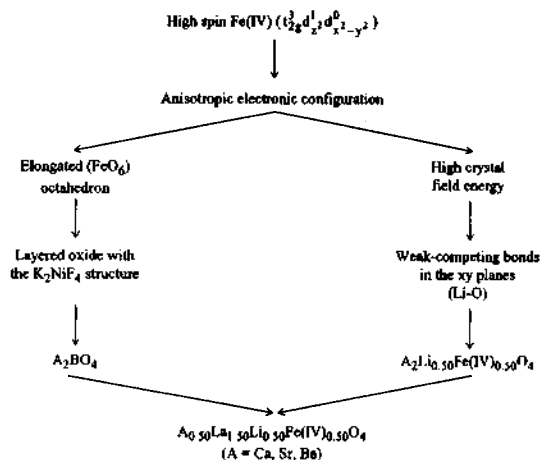


Fig. 6. The different criteria characterizing the local surrounding of Fe(IV) and leading to the selection of an appropriate stoichiometry.

The physical characterizations confirm the stabilization of Fe(IV) with the high spin state ($t_{2g}^3 d_{xy}^2$) (Table 6). More recently, others phases with the K_2NiF_4 -type structure and containing Fe(IV) with the high spin state have been prepared.^{21,22}

THE STABILIZATION OF Cu(III)

Before the discovery of new high T_c superconducting oxides containing Cu(III) this unusual oxidation state was practically unknown. As soon as 1970 using the criteria previously described, Cu(III) was stabilized in two main lattices: LaCuO_3 with the perovskite structure and $\text{La}_2\text{Li}_{0.50}\text{Cu}_{0.50}\text{O}_4$ with the K_2NiF_4 one.²³

Taking into account the strong covalency of the chemical bond Cu(III)-O, it was possible to propose for Cu(III) (d^8) two different electronic configurations in a six-coordinated polyhedron: (i) $t_{2g}^6 e_g^2$ with a delocalization of the e_g electrons in a σ^* band; (ii) d^8 low-spin ($t_{2g}^6 d_{xy}^2 d_{x^2-y^2}^0$) with localized electrons.

The perovskite LaCuO_3 was firstly prepared under high oxygen pressure in a belt type equipment using KClO_3 as oxygen source ($P \approx 7$ GPa, $T = 900^\circ\text{C}$) with the rhombohedral distortion.^{23,24} Recently new investigations have pointed out that a tetragonal form can be stabilized at lower pressures ($P < 5$ GPa).²⁵ On the contrary, $\text{La}_2\text{Li}_{0.50}\text{Cu}_{0.50}\text{O}_4$ have been prepared at lower oxygen pressure $P \approx 400$ MPa. If Cu(III) adopts the first configuration ($t_{2g}^6 e_g^2$) in the perovskite LaCuO_3 characterized by a Pauli paramagnetism,²⁴ on the contrary the second one (d^8 low-spin) is observed in $\text{La}_2\text{Li}_{0.50}\text{Cu}_{0.50}\text{O}_4$ with diamagnetic properties. These two materials can be considered as the limits of the behaviour of Cu(III) in an oxygen lattice.

CONCLUSIONS

High oxygen pressures was, during these last thirty years mainly developed in two directions:

- (i) the synthesis of new oxides at high temperatures from thermally unstable reactants,
- (ii) the stabilization of unusual oxidation states of transition metals.

The second route was strongly investigated in Bordeaux. These research works have led to the characterization of different new oxidation states as Cu(III), Fe(V), Ir(V), Ir(VI), or electronic configurations as high spin Fe(IV) ($t_{2g}^4 d_{z^2} d_{x^2-y^2}^2$) or Co(III) with an intermediate electronic configuration ($d_{xy}^2 d_{xz}^2 d_{yz}^2 d_{z^2} d_{x^2-y^2}^1$). Such developments has allowed to evaluate (i) the evolution of the M^{n+} -O distance versus the $n+$ value and (ii) the t_{2g} - e_g splitting.

REFERENCES

1. Demazeau, G. *Thesis doctorates Sciences*; University of Bordeaux, 1973.
2. Tanabe, Y.; Sugano, S. *J. Phys. Soc. Japan*. **1954**, *9*, 753.
3. Krishnamurthy, R.; Schaap, W. B. *J. Chem. Educ.* **1969**, *46*, 799.
4. Buffat, B. *Thesis doctorates Sciences*; University Bordeaux I, 1984; n^o802.
5. Buffat, B.; Demazeau, G.; Pouchard, M.; Hagenm ller, P. *Proc. Indian Acad. Sc (Chem. Sci.)*, **1984**, *93(3)*, 313.
6. Demazeau, G.; Buffat, B.; Menil, F.; Fourn s, L.; Pouchard, M.; Dance, J. M.; Fabritchnyi, P.; Hagenm ller, P. *Mat. Res. Bull.* **1991**, *16*, 1465.
7. M ler, R. A.; Th Von Waldkirch and W. Berlinger, *Solid State Comm.* **1971**, *9*, 1097.
8. Choy, J. H.; Demazeau, G.; Byeon, S. H. *Solid State Comm.* **1991**, *77(9)*, 647.
9. Shannon, R. D. *Acta Cryst.* **1976**, *A32*, 751.
10. Jung, D. Y. *Thesis of the University Bordeaux I*; 1995; n^o1313.
11. Demazeau, G.; Jung, D. Y.; Sanchez, J. P.; Blaise, A. Fourn s, L. *Solid State Comm.* **1993**, *85(6)*, 479.
12. Jung, D. Y.; Gravereau, P.; Demazeau, G. *Eur. J. Solid State and Inorg. Chem.* **1993**, *30*, 1025.
13. Demazeau, G.; Jung, D.Y. *Eur. J. Solid State and Inorg. Chem.* **1995**, *32*, 383.
14. Jung, D. Y.; Demazeau, G. *J. Solid State Chem.* **1995**, *115*, 447.
15. Jung, D. Y.; Demazeau, G.; Etourneau, J.; Subramanian, M. A. *Mat. Res. Bull.* **1995**, *30(1)*, 113.
16. Choy, J. H.; Kim, D. K.; Hwang, S. H.; Demazeau, G.; Jung, D. Y. *J. Am. Chem. Soc.* **1995**, *117*, 8557.
17. Demazeau, G.; Pouchard, M.; Chevreau, N.; Colombet, J. F.; Thomas, M.; Menil, F.; Hagenm ller, P. *C. R. Acad. Sci.* **1980**, *290*, 177.
18. Demazeau, G.; Pouchard, M.; Chevreau, N.; Colombet, J. F.; Thomas, M.; Menil, F.; Hagenm ller, P. *J. Less Common Metals* **1980**, *76*, 279.
19. Demazeau, G.; Chevreau, N.; Fourn, L.; Soubeyroux, J. L.; Takeda, Y.; Thomas, M.; Pouchard, M. *Rev. Chim. Miner* **1983**, *20*, 155.
20. Soubeyroux, J. L.; Chevreau, N.; Demazeau, G.; Pouchard, M.; Hagenm ller, P. *J. Solid State Chem.* **1984**, *51*, 38.
21. Zhu, L. M.; Demazeau, G.; Fourn s, L.; Pouchard, M.; Hagenm ller, P. *C. R. Acad. Sci., S rie II* **1987**, *304(12)*, 633.
22. Demazeau, G.; Zhu, L. M.; Fourn s, L.; Pouchard, M.; Hagenm ller, P. *J. Solid State Chem.* **1988**, *72*, 31.
23. Demazeau, G.; Parent, C.; Pouchard, M.; Hagenm ller, P. *Mat. Res. Bull.* **1972**, *7*, 913.
24. Goodenough, J. B.; Mott, N. F.; Pouchard, M.; Demazeau, G.; Hagenm ller, P. *Mat. Res. Bull.* **1973**, *8*, 647.
25. Darracq, S.; Largeteau, A.; Demazeau, G.; Scott, B. A.; Bringley, J. F. *Eur. J. Solid State and Inorg. Chem.* **1992**, *29*, 585.